Global-phase seismic interferometry unveils P-wave reflectivity below the Himalayas and Tibet — auxiliary material

Elmer Ruigrok, Shu-Huei Hung and Kees Wapenaar

April 24, 2012

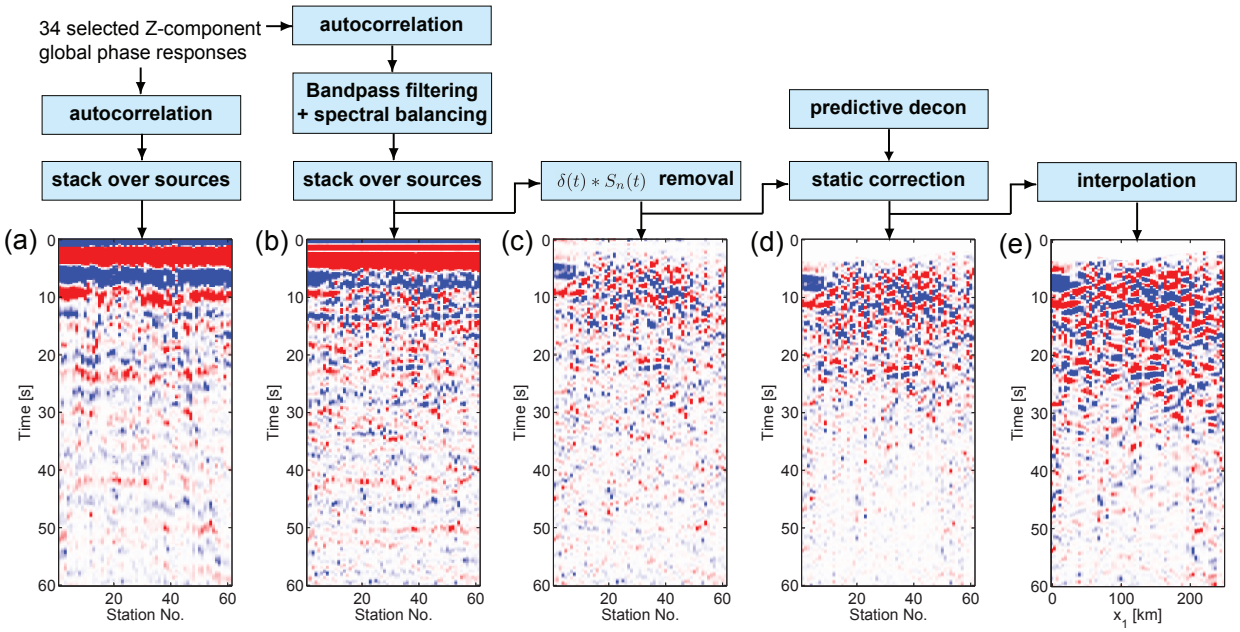

Figure A.1: 5 stages of the estimated zero-offset reflection response below the Himalaya array (light-green line in Fig. A.2). From left to right (a–e), the estimation of the primary reflection response is improved by a succession of pre- and postprocessing algorithms (see text in main document). The used algorithms are indicated on top of the zero-offset panels, in the form of a flowchart.

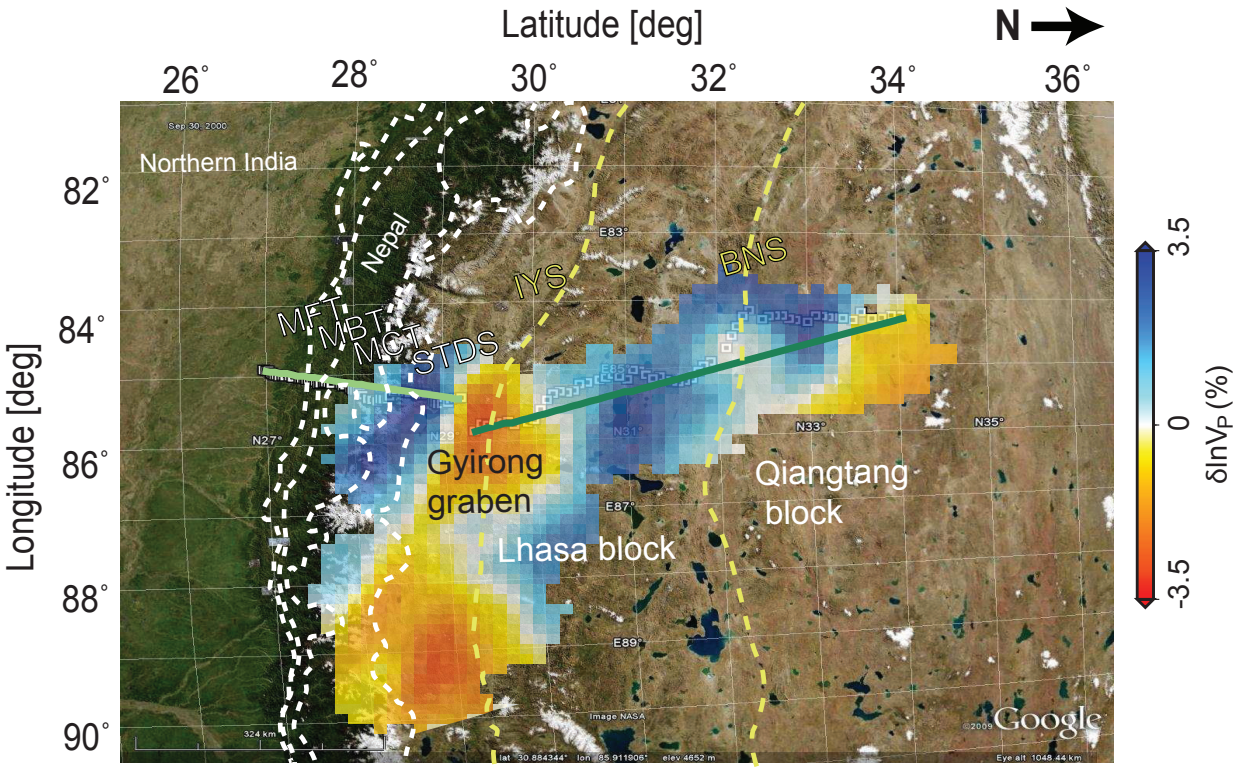

Figure A.2: A satellite image of the Central Himalayas and Central Tibetan Plateau, showing seismic stations (white squares with black dots) from the Hi-CLIMB experiment [e.g, *Nábělek et al.*(2009);*Nowack et al.*(2010)]. The station distribution is split into two subarrays, the Himalaya and the Tibet array. The linearized Himalaya and Tibet arrays are indicated with a light-green and dark-green line, respectively. The dashed white lines denote the major shear zones related to the formation of the Himalayas: MFT (Main Frontal Thrust), MBT (Main Boundary Thrust), MCT (Main Central Thrust) and STDS (South Tibetan Detachment System). The dashed yellow lines denote the suture zones related to the formation of the Tibetan Plateau: IYS (Indus Yarlung Suture) and BNS (Banggong Nujiang Suture) [e.g, *Yin and Harrison*, 2000]. The satellite image is overlain by a slice, taken at 56 km depth, from the P-wave velocity-anomaly model, as obtained by multiscale finite-frequency traveltime tomography [*Hung et al.*, 2011]. The model shows the Gyirong Graben as a low-velocity anomaly straddling around the IYS, just north of the Himalayas. Around the other old suture zone, the BNS, a much weaker velocity anomaly can be identified.

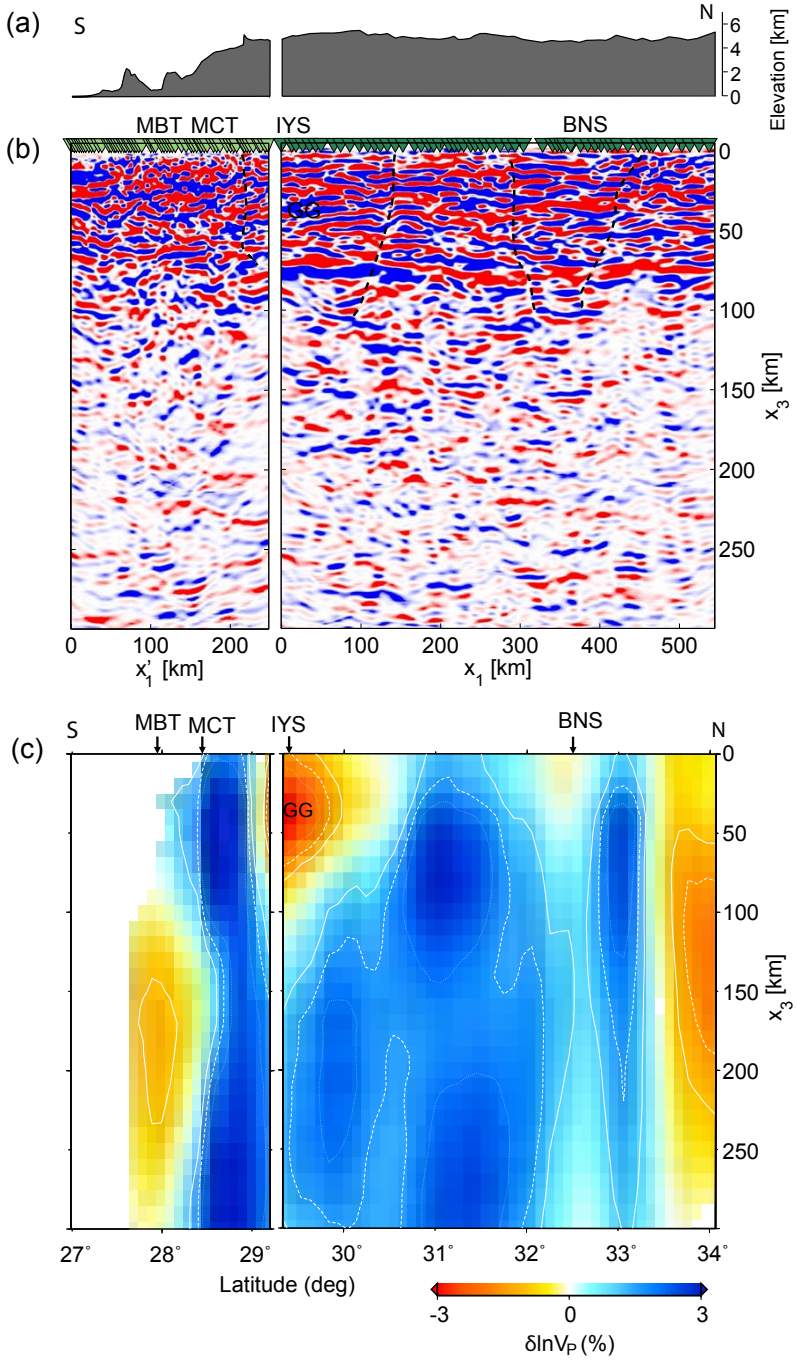

Figure A.3: (a) The topography below (left) the Himalaya array and (right) the Tibet array. For a map view of these seismic arrays, see Figure A.2. (b) The obtained P-wave reflectivity images for the two arrays. The reflectivity images were obtained by the application of global-phase seismic interferometry and migration (see main text). The reflectivity images are compared with (c) two P-wave velocity-anomaly sections from the same locations. The latter sections were sliced from a 3D tomographic model [*Hung et al.*, 2011]. Both on the reflectivity image and the tomographic image, the development of graben structures can be noted. On the reflectivity images, the limiting faults of the Gyirong Graben (GG), and the rifting zone around the Banggong Nujiang Suture (BNS), are identified by discontinuities in reflectivity in the crust (indicated with the dashed black lines). On the tomographic images, the weak zones along which east-west extension takes place are imaged as low-velocity anomalies in the crust. For the meaning of the undefined abbreviations in the figure (MBT, MCT and IYS), see Figure A.2.